Chapter 11. Injection

C. Ankenbrandt, A. Drozhdin, C. Johnstone, O. Krivosheev, J. Lackey, C. Prior

11.1. Introduction

There are three 63.921 m long straight sections in the ring. One of them with 17 m of preceding arc, called together "utility section", is used for beam injection and collimation [1]. Two other long straight sections are used for RF cavities and extraction. The Proton Driver beta functions and dispersion along the utility section are shown in Fig. 11.1.

Table 11.1. Proton Driver parameters.

Kinetic energy at injection	0.4 GeV
Injected beam normalized transverse emittance	3 mm.mrad
Normalized transverse emittance after painting	60 mm.mrad
Painting injection duration	90 μs (27 turns)
Total intensity at injection	3.3×10^{13}
Horizontal betatron tune	11.43
Vertical betatron tune	12.38
Horizontal β at the foil	22.895 m
Horizontal α at the foil	-0.256
Horizontal dispersion at the foil	0.013 m
Vertical β at the foil	9.231 m
Vertical α at the foil	0.002
Horizontal beam size at injection in the foil	σ_x= 3.35 mm
Vertical beam size at injection in the foil	σ_y= 2.13 mm

The beam halo collimation system [2] is used to localize proton losses in a specially shielded short section of the utility section, and so to reduce irradiation the rest of the ring to an acceptable level. It consists of two primary and several secondary collimators located in drift spaces in the first 50 m of the utility section.

Painting injection is required to realize uniform density distributions of the beam in the transverse plane for space charge effect reduction. This preserves emittance at injection. Table 11.1 represents the Proton Driver parameters [3] that are relevant the painting system design.

11.2. Painting Injection Scheme

Painting injection is performed by using two sets of fast horizontal and vertical magnets (kickers). The proton orbit is moved in the horizontal plane at the beginning of injection by 52 mm to the thin graphite stripping foil to accept the first portion of protons generated by H^- in the foil (Fig. 11.2). Four 0.5 m long kicker magnets are used to produce orbit

displacement (Fig. 11.3). The maximum field of the kicker magnets is 0.21 kG. The horizontal kick at the beginning of beam painting is shown in Fig. 11.4. Gradual reduction of kicker strength permits "painting" the injected beam across the accelerator aperture with the required emittance. Vertical kicker magnets located in the injection line (not shown here) provide injected beam angle sweeping during injection time, starting from maximum at the beginning of injection and going to zero at the end of painting process. Horizontal and vertical kickers produce particle betatron amplitude variation during injection. This results in a uniform distribution of the circulating beam after painting. Painting starts from the central region of phase space in the horizontal plane and from the border of it in the vertical plane, and goes to the border of the beam in the horizontal plane and to to the center in the vertical plane. This produces a so called "uncorrelated beam" with elliptical cross section,thereby eliminating particles that have maximum amplitudes in both planes simultaneously.

A septum-magnet located upstream of the foil (Fig. 11.3) is used to separate the proton and H^- beams at the quadrupole upstream of the foil by 700 mm. This allows the H^- beam to pass outside the quadrupole body. The beam dump located behind the stripping foil is used for H^o interception. Injection kickers cause negligible perturbation of the β functions and dispersion at injection (Fig. 11.4). Horizontal dispersion in the foil at injection is equal to -0.013 m.

Multi-turn particle tracking through the accelerator is done with the STRUCT [4] code. A stripping foil made of 300 μg/cm^2 (1.5 μm) thick graphite has the shape of so-called corner foil, where two edges of the square foil are supported and the other two edges are free. The foil size is 2.6 cm $\times$ 3.8 cm.

The dependence of kicker-magnets strength on time is chosen to get uniform distribution of the beam after painting both in horizontal and vertical planes. An optimal waveform of bump-magnets [5] was simulated in the STRUCT code as presented below:

- in the horizontal plane

$$B = B_o \left[0.4873 + 0.5127 \left(1 - \sqrt{\frac{2\,N}{27} - \left(\frac{N}{27}\right)^2} \right) \right] \qquad N < 27 \tag{11.1}$$

$$B = B_o \left[0.4873 - \frac{N - 27}{12.3127} \right] \qquad N > 27 \tag{11.2}$$

- in the vertical plane

$$Y' = Y'_o \sqrt{2\frac{27 - N}{27} - \left(\frac{27 - N}{27}\right)^2} \qquad Y'_o = 1.835\ mrad \tag{11.3}$$

Here N is the turn number from beginning of painting.

Horizontal phase plane of injected beam in the foil is shown in Fig. 11.5. Emittance of injected beam at 95% is equal to 3 mm·mrad.

Painting lasts during 27 turns, and after painting the circulating beam moves out of the foil during 6 turns. In the simulations the horizontal bump amplitude at the foil is 52 mm =

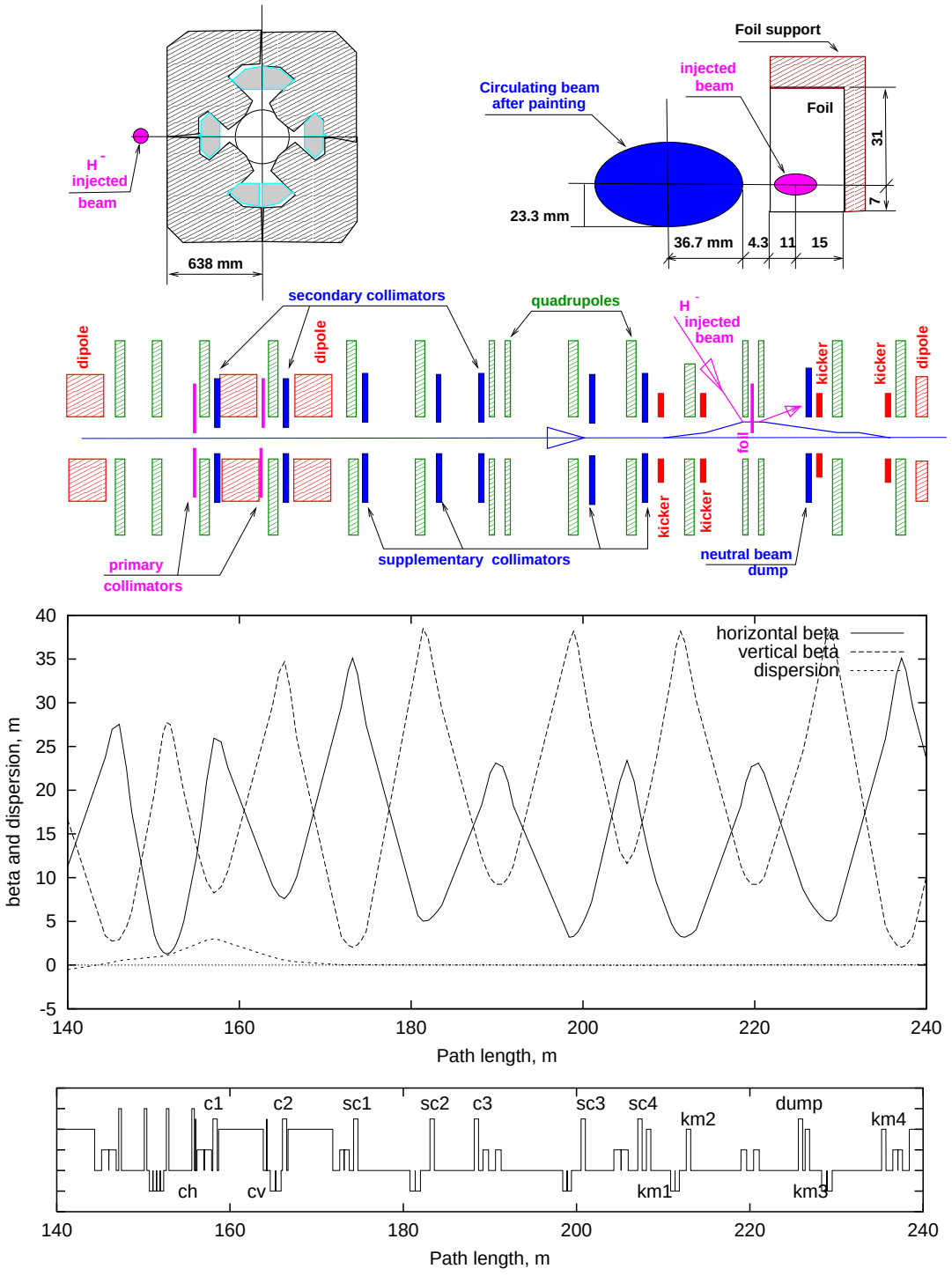

Figure 11.1. Beam collimation and beam painting systems (top) and beta functions and dispersion in the utility section (bottom).

26.7 mm (painting) + 25.3 mm (removing from the foil) (Fig. 11.2). Vertical angle variation is 1.835 mrad. Horizontal and vertical phase plane of circulating beam in the foil at 6-th, 28-st, and 33-d turns from the beginning of beam painting are presented in Fig. 11.6.

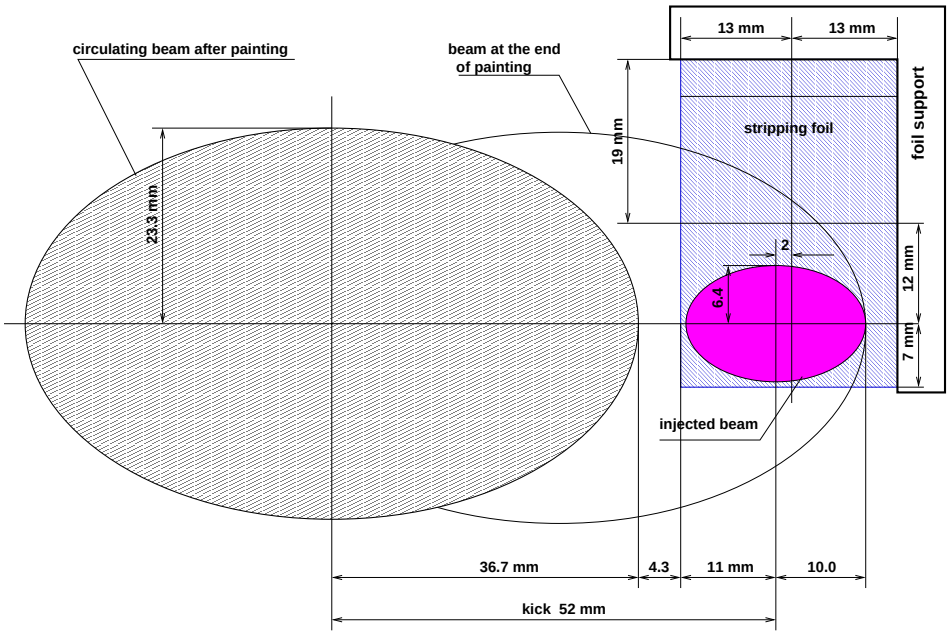

Figure 11.2. Injected and circulating beams location in the foil at painting.

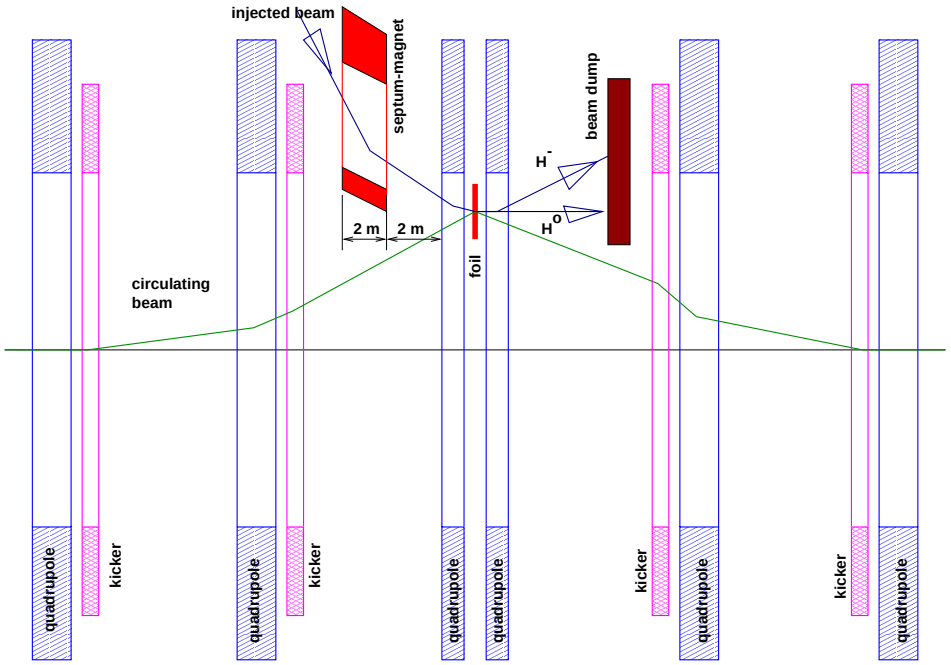

Figure 11.3. Painting injection scheme.

Horizontal kicker-magnet strength and vertical angle of the beam in the foil during injection are presented in the top of Fig. 11.7. Particle transverse population and particle density distribution after painting at the foil location are shown in the middle and at the bottom of Fig. 11.7. Injected beam at the foil and circulating beam after painting in a horizontal phase plane are shown in Fig. 11.7.

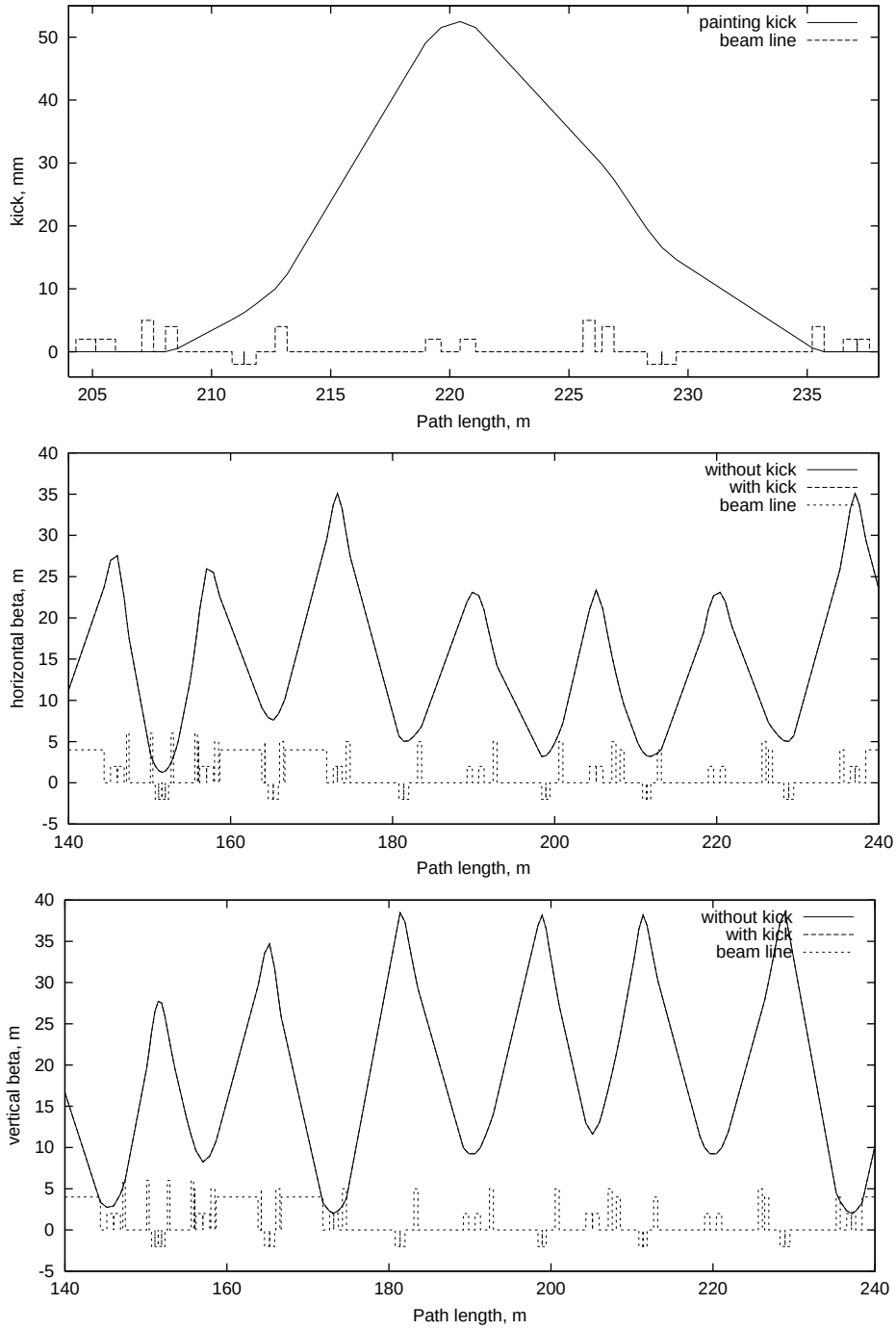

Figure 11.4. Horizontal kick for beam painting (top). Horizontal (middle) and vertical (bottom) beta functions with and without painting bump and kick.

Average number of hits upon the stripping foil for each particle is as low as 1.98. This effects low-level nuclear interactions and multiple Coulomb scattering in the foil at injection, and because of this causes low-level particle loss at injection.

The circulating protons pass several times through the foil and some of them can be lost

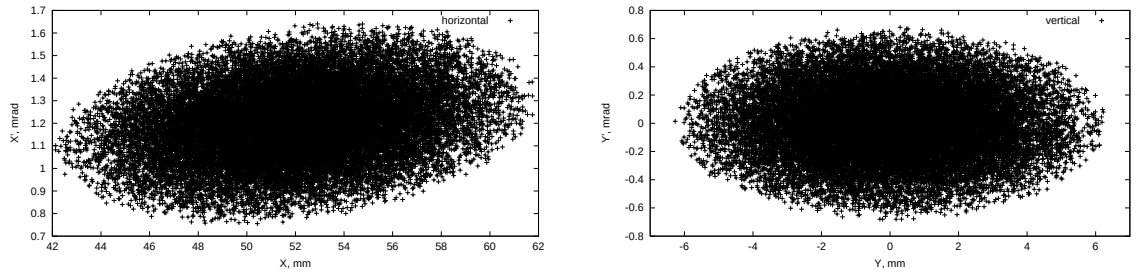

Figure 11.5. Horizontal (left) and vertical (right) phase plane in the foil at injection.

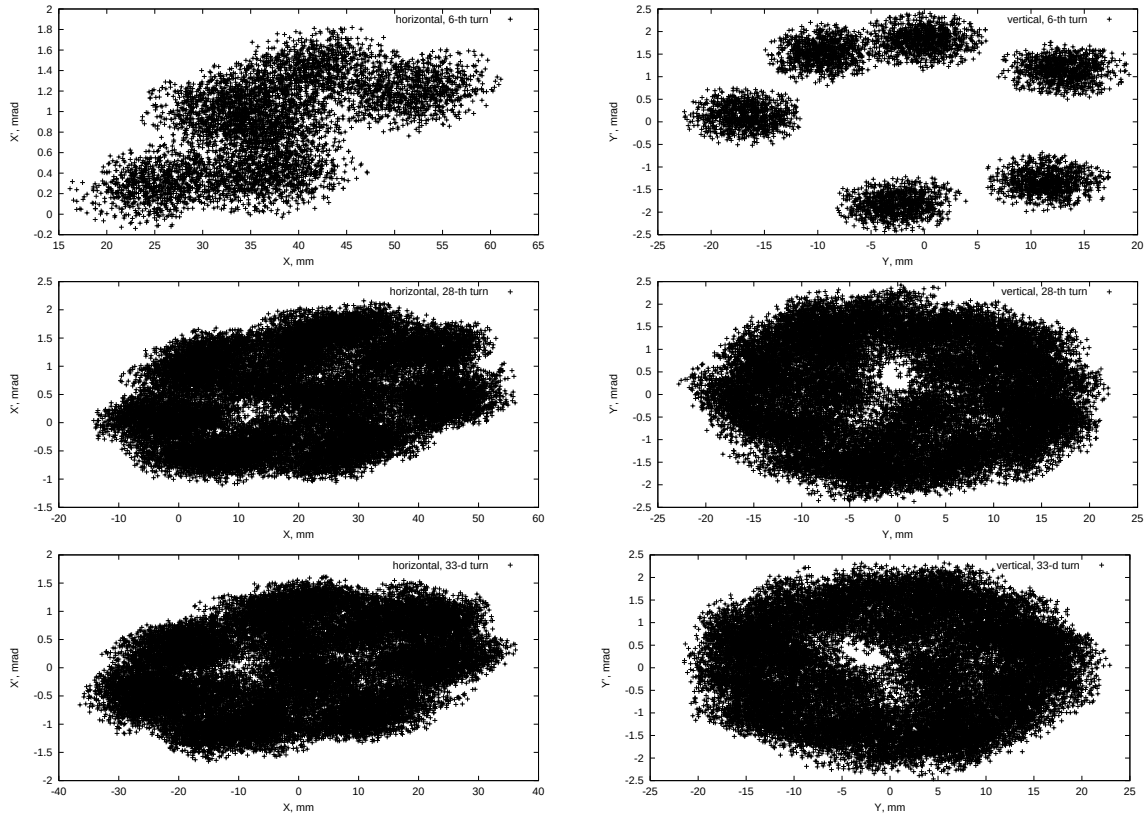

Figure 11.6. Horizontal (left) and vertical (right) phase plane in the foil at 6-th (top), 28-th (middle), and 33-d (bottom) turn from the beginning of beam painting.

because of scattering in the foil. Multiple Coulomb scattering is very small because of small foil thickness. Particle energy loss in the foil at one pass is $2.4{\cdot}10^{-6}$ of initial energy. The rate of nuclear interactions in the foil during the total process is $1.0{\cdot}10^{-5}$ of the injected intensity. The emittance of the circulating beam in the horizontal plane is small in the beginning of painting and it gradually reaches maximum only at the end of painting. Therefore particle horizontal amplitude, in average, is sufficiently less compared to the accelerator aperture. Particles can be lost only during the first few turns after injection, and only in the region of injection kick maximum where the beam is close to accelerator aperture. At every next turn after particles are injected, they move away from the aperture restriction because of fast reduction of painting kick amplitude. Simulations shown that the rate of particle loss

in the accelerator at interaction with foil is as low as $7.4{\cdot}10^{-5}$ of the injected intensity.

11.3. Stripping Foil

We developed and used an analytical approach for calculating the foil temperature after painting injection and after many passes of proton beam through the foil. In this section, we describe the method of calculation of the foil temperature after it reaches a quasi-steady state.

Standard notation is applied below, namely:

- c - the speed of light,
- $\hbar$ - the Planck constant,
- k - the Boltzmann constant,
- $m_e c^2$ - the electron rest mass,
- r_e - the electron classical radius,
- N_a - the Avogadro number,
- $\sigma_{SB} = \pi^2 k^4 / 60\hbar^3 c^2$ is the Stefan-Boltzmann constant,
- M and E are proton mass and energy,
- γ - the Lorentz-factor,
- β - the proton speed in the units of c,
- N - the number of particles injected per turn,
- σ_x and σ_y are r.m.s. for Gaussian distribution of injected beam at the foil,
- A, Z and I are the mass, charge and ionization potential of target material,
- ρ and c_p are the material density and the specific heat,
- κ and ε are the material thermal conductivity and the emissivity.

11.3.1. Deposited Energy

We consider that contributions from nuclear reactions are negligible. The only energy deposition, and therefore heating source, would be the ionization energy loss in the foil. The density of energy deposited during one injection pulse is:

$$S(\vec{r},t) = \frac{N}{2\pi\sigma^2} \cdot |\frac{dE}{dz}| \cdot e^{-r^2/2\sigma^2} \cdot \delta(t) \tag{11.4}$$

where $\delta(t)$ is Dirac's delta-function. It is properly normalized, so that the total energy deposition is

$$S_{total} = \int_V d^3\vec{r} \int dt\, S(\vec{r},t) = N \cdot |\frac{dE}{dz}| \cdot \Delta z$$

where Δz is the foil thickness. From "Review of Particle Properties" [6] the ionization energy loss - the main energy deposition source in the case of thin foil - can be written as the Bethe-Bloch equation:

$$-\frac{dE}{dz} = K \cdot \frac{Z}{A} \cdot \frac{1}{\beta^2} [\frac{1}{2} \log \frac{2m_e c^2 \beta^2 \gamma^2 T_{max}}{I^2} - \beta^2 - \frac{1}{2}\delta] \tag{11.5}$$

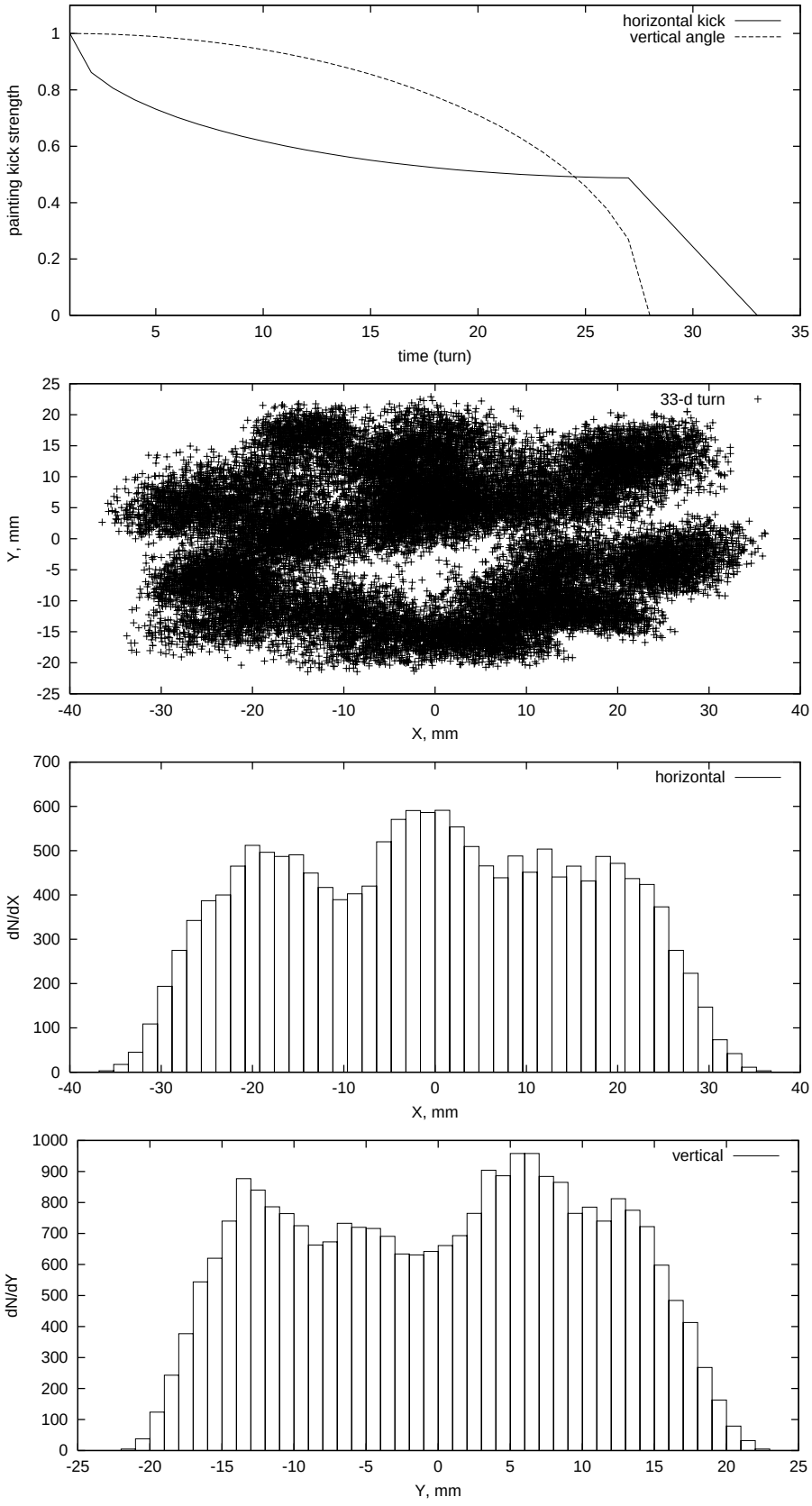

Figure 11.7. Horizontal kicker strength and vertical angle of the beam at injection in the foil (top). Particle transverse population (middle) and particle density distribution in the foil (bottom) at 33-d turn from the beginning of beam painting.

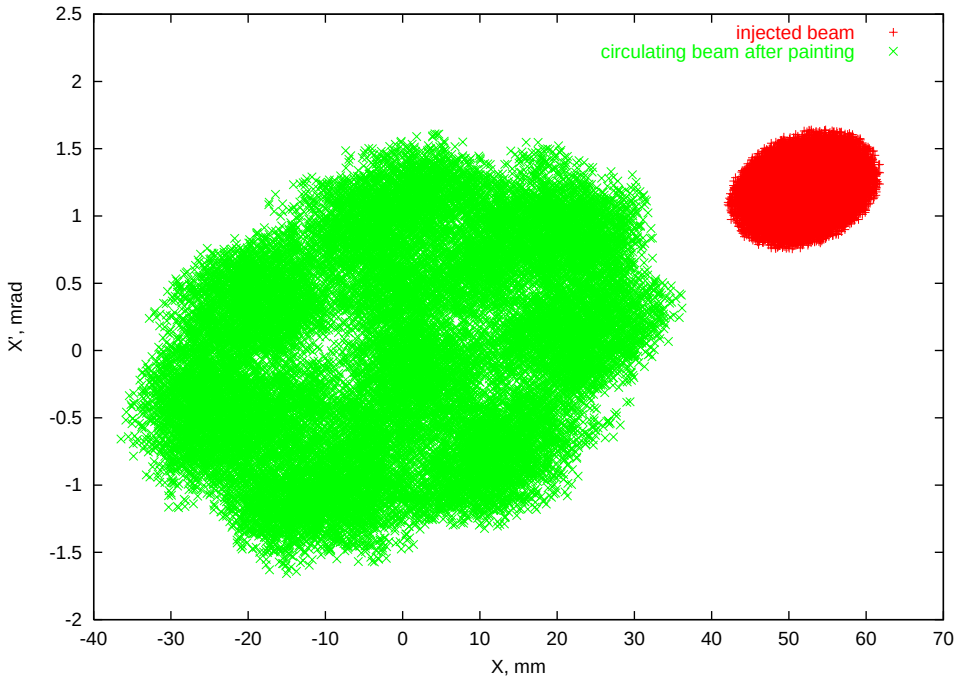

Figure 11.8. Injected beam at the foil and circulating beam after painting.

where $K = 4\pi N_a r_e^2 m_e c^2 = 0.307075 \frac{MeV \cdot cm^2}{g}$. T_{max} is the maximum energy transfer in one collision, and for foils it is smaller than the kinematically allowed maximum energy transfer

$$T_{max} = \frac{2m_e c^2 \beta^2 \gamma^2}{1 + 2\gamma m_e / M + (m_e/M)^2}.$$

and δ is density correction, calculated according to the Sternheimer approximation.

11.3.2. Beam Painting and Foil Heating

Because the foil thickness is quite small, we consider the heat propagation from heated area to the edges, where it could be collected and moved away, quite small, so we concentrated our efforts on the heat loss due to emission.

Heat Emission

Another way to dissipate heat after the injection pulse is by radiation. The energy emission of the black body is proportional to the temperature to the fourth power, according to the Stefan-Boltzmann law:

$$Q = \sigma_{SB} \cdot T^4.$$

The Stefan-Boltzmann law is approximately true for the foil if we include the material emissivity ε. Therefore, the heat propagation equation with emission as the only mechanism to cool the foil is

$$\frac{\partial T}{\partial t} = \frac{S(\vec{r},t)}{\rho c_p} - \frac{\varepsilon \sigma_{SB}}{\Delta z \rho c_p} \cdot (T^4 - T_0^4), \tag{11.6}$$

We will solve (11.6) in two steps. First consider the time interval from zero to very small ε. Emission did not change the temperature, therefore the only variable will be the source term and after integration over t from zero to ε we have:

$$T_\varepsilon = T_0 + \frac{1}{\rho c_p}\frac{N}{2\pi\sigma^2}\left|\frac{dE}{dz}\right| e^{-r^2/2\sigma^2}. \tag{11.7}$$

Then we solve the equation

$$\frac{\partial T}{\partial t} = -\frac{\varepsilon\sigma_{SB}}{\Delta z\rho c_p}\cdot(T^4 - T_0^4), \tag{11.8}$$

starting from time ε and using T_ε (11.7) as initial value. Integration of (11.8) gives us the equation for $T(t)$ dependence:

$$-\frac{\varepsilon\sigma_{SB}}{\Delta z\rho c_p}(t-\varepsilon) = \frac{1}{2T_0^3}[\arctan\frac{T_\varepsilon}{T_0} - \arctan\frac{T}{T_0}] + \frac{1}{4T_0^3}[\log\frac{T-T_0}{T_\varepsilon - T_0} - \log\frac{T+T_0}{T_\varepsilon + T_0}]. \tag{11.9}$$

In order to solve (11.6) it is obvious we have to obtain the limit $\varepsilon \to 0$. Such limit only removes ε from the right part of equation (11.8). For clarify, we provide the explicit dependence in the next equation

$$t = \frac{\Delta z\rho c_p}{2T_0^3\varepsilon\sigma_{SB}}[\arctan\frac{T_0(T(\vec{r},t) - T_\varepsilon(\vec{r}))}{T_0^2 + T_\varepsilon(\vec{r})T(\vec{r},t)} + \frac{1}{2}\log\frac{(T_\varepsilon(\vec{r}) - T_0)\cdot(T(\vec{r},t) + T_0)}{(T_\varepsilon(\vec{r}) + T_0)\cdot(T(\vec{r},t) - T_0)}]. \tag{11.10}$$

But it is probably impossible to get an explicit dependence $T(\vec{r},t)$ trying to reverse (11.9). Therefore numerical solution is required.

To find a temperature behavior at injection when pulses follow each other with τ seconds between them, is easy to write down the recursive procedures for the temperature at a given time

$$\begin{aligned}
T_{j\tau} &= T_{\varepsilon+(j-1)\tau}\cdot\sqrt[3]{\frac{\Delta z\rho c_p}{3\varepsilon\sigma_{SB}T^3_{\varepsilon+(j-1)\tau}\cdot\tau + \Delta z\rho c_p}},\\
T_{j\tau+\varepsilon} &= T_{j\tau} + \frac{N}{2\pi\sigma^2\rho c_p}\left|\frac{dE}{dz}\right|\exp(-\vec{r}^2/2\sigma^2),\\
T(j\tau < t < (j+1)\tau) &= T_{j\tau+\varepsilon}\cdot\sqrt[3]{\frac{\Delta z\rho c_p}{3\varepsilon\sigma_{SB}T^3_{j\tau+\varepsilon}\cdot t + \Delta z\rho c_p}}.
\end{aligned}$$

The same scheme can be written for $T(t)$ dependence when T_0 is not equal to 0, but from (11.10) it is obvious that $T_{j\tau}$ and $T(j\tau < t < (j+1)\tau)$ can be obtained only numerically.

Foil Temperature Rise

We consider the temperature rise due to multiple passage of protons through the foil to be instantaneous. Now we have to derive the expression which describes the particle and heat

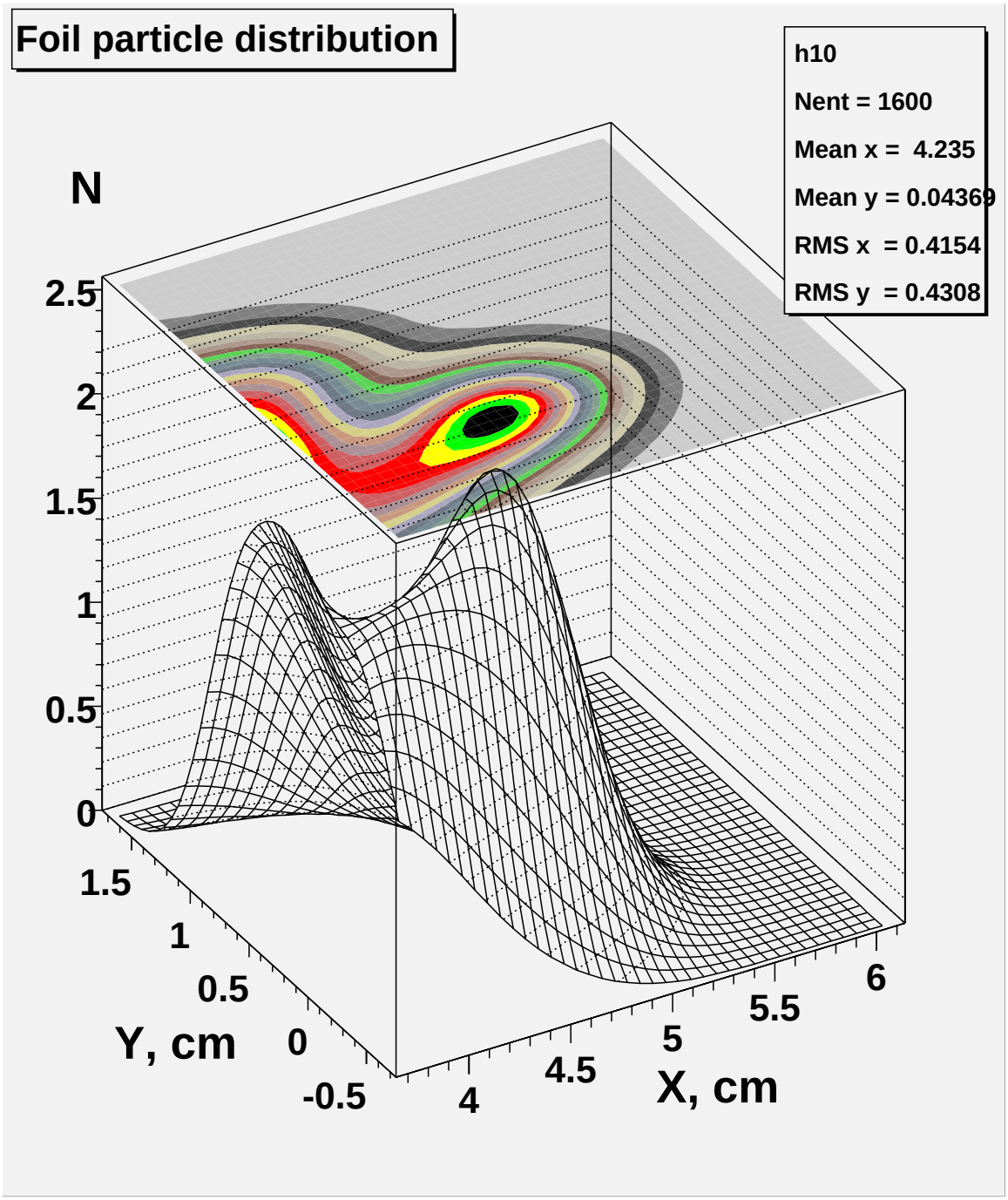

Figure 11.9. Proton hits distribution upon the stripping foil at painting injection.

distribution on the foil during the painting cycle. The following notation is used: x_n^k and y_n^k are the center of injected bunch. Index k is the turn index while n denotes the injection index. There are some conditions on k and n, namely $0 \leq n \leq N_c = 27$ and $n \leq k \leq N_c + N_f$, where N_f is the number of turns for beam removal from the foil at the end of injection. The

circulating orbit position resulting from equations (11.1, 11.2) is given by:

$$\begin{aligned} x_k^o &= x_0\{p_0 + p_1 \cdot [1 - \sqrt{\frac{2k}{N_c} - (\frac{k}{N_c})^2}]\} \qquad N \le 27 \\ x_k^o &= x_0 \cdot p_0\{1 - \frac{k - N_c}{N_f}\} \qquad N > 27 \\ y_k^o &= 0 \end{aligned}$$

where p_0 and p_1 denote orbit position at the end of painting and amplitude of the closed orbit bump during the painting process. Obviously, $p_0 + p_1 \equiv 1$. As was mentioned, painting starts from the center of the beam in the horizontal plane and from large amplitude in the vertical plane, producing an elliptical cross section for the circulating beam. The beam is injected in the ellipse with transverse amplitudes (11.3) of

$$\begin{aligned} x_n^e &= p_1 \cdot x_0 \cdot \sqrt{\frac{2n}{N_c} - (\frac{n}{N_c})^2} \\ y_n^e &= y_0 \sqrt{2 \cdot \frac{N_c - n}{N_c} - (\frac{N_c - n}{N_c})^2} \end{aligned}$$

We now can write down the expression for x_n^k and y_n^k. Knowing the horizontal and vertical tunes ν_x and ν_y

$$\begin{aligned} x_n^k &= x_k^o + x_n^e \cdot \cos[2\pi\nu_x(k-n)] \\ y_n^k &= y_k^o + y_n^e \cdot \cos[2\pi\nu_y(k-n) - \pi/2] \end{aligned}$$

and if we define N_i as number of particles injected in one cycle, the proton density $S_N(\vec{r},t)$ will be

$$S_N(\vec{r},t) = \frac{N_i}{2\pi\sigma_x\sigma_y} \sum_{n=0}^{N_c} \sum_{k=n}^{N_c+N_f} e^{-(x-x_n^k)^2/2\sigma_x^2 - (y-y_n^k)^2/2\sigma_y^2}$$

and for a foil with left lower corner (x_{ll}, y_{ll}) and upper right corner (x_{ur}, y_{ur}) we can get the average number of collisions as the result of integration

$$< N_{col} >= \frac{1}{N_c \cdot N_i} \int_{x_{ll}}^{x_{ur}} dx \int_{y_{ll}}^{y_{ur}} dy\, S_N(\vec{r},t)$$

Integrating this one can get

$$\begin{aligned} < N_{col} > &= \sum_{n=0}^{N_c} \sum_{k=n}^{N_c+N_f} [erf(\frac{x_{ur} - x_n^k}{\sqrt{2}\sigma_x}) + erf(\frac{x_n^k - x_{ll}}{\sqrt{2}\sigma_x})] \cdot \\ &\quad [erf(\frac{y_{ur} - y_n^k}{\sqrt{2}\sigma_y}) + erf(\frac{y_n^k - y_{ll}}{\sqrt{2}\sigma_y})]/4N_c \end{aligned}$$

Next a very similar expression gives us the total energy deposited in the foil:

$$\begin{aligned} E_{tot} &= \frac{\Delta z}{4N_c} \sum_{n=0}^{N_c} \sum_{k=n}^{N_c} [|\frac{dE_p}{dz}| + 2|\frac{dE_e}{dz}|\delta_{n,k}][erf(\frac{x_{ur} - x_n^k}{\sqrt{2}\sigma_x}) + \\ &\quad erf(\frac{x_n^k - x_{ll}}{\sqrt{2}\sigma_x})][erf(\frac{y_{ur} - y_n^k}{\sqrt{2}\sigma_y}) + erf(\frac{y_n^k - y_{ll}}{\sqrt{2}\sigma_y})] \end{aligned}$$

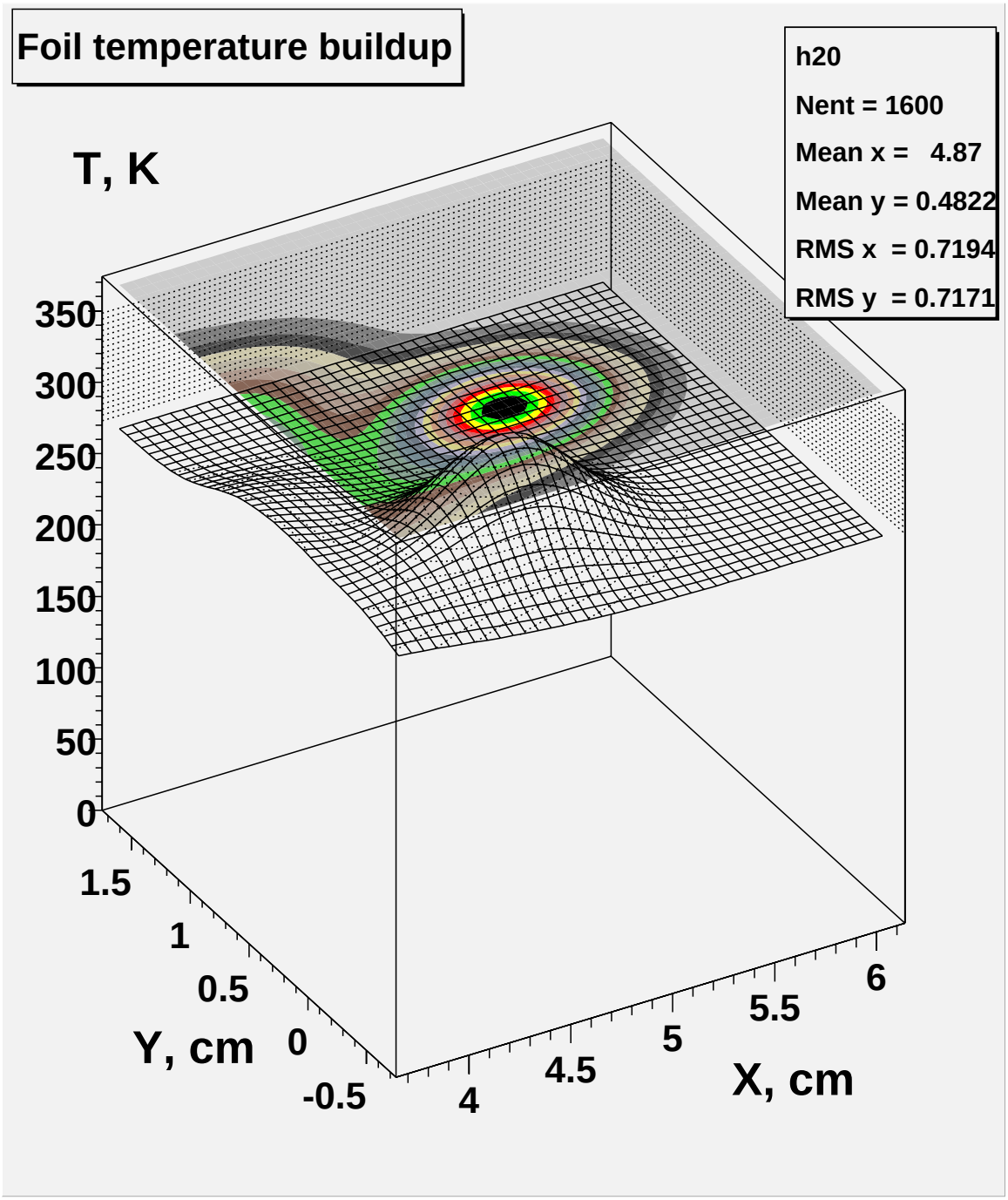

Figure 11.10. Stripping foil temperature buildup after one cycle of particles injected into the proton driver.

If we have both heat emission and heat transfer the equations become more complicated. Combining heat transfer and emission together, one can get

$$\frac{\partial T}{\partial t} = a(\vec{\nabla}^2 T) + \frac{S(\vec{r},t)}{\rho c_p} - \frac{\varepsilon \sigma_{SB}}{\Delta z \rho c_p} \cdot (T^4 - T_0^4), \qquad (11.11)$$

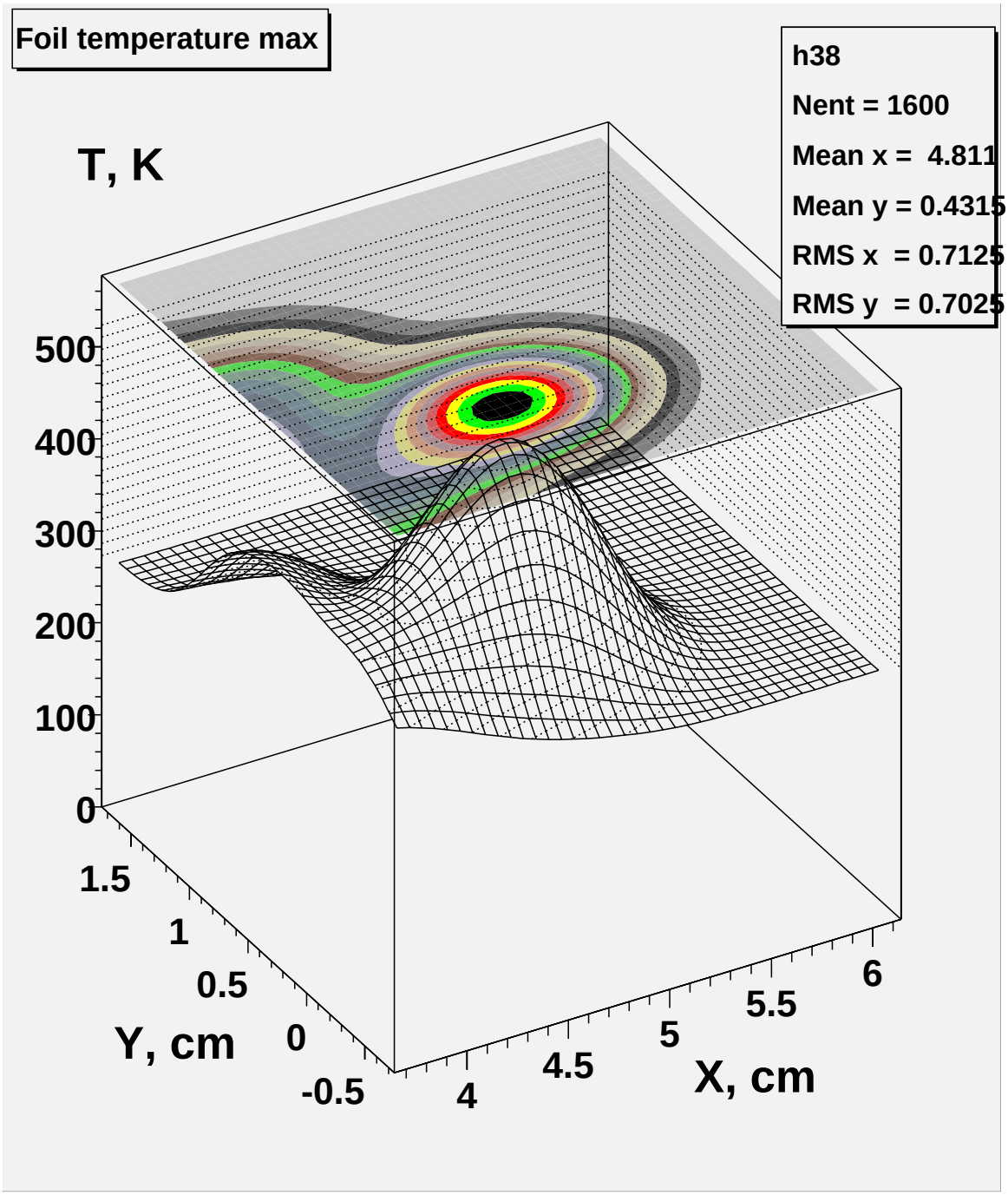

Figure 11.11. Steady state maximum temperature distribution in the stripping foil at painting injection to the proton driver.

The only way to solve such an equation is numerically, using a code such as ANSYS [7]. Because we estimate the heating and cooling of the foil using only emission, then our calculation should be viewed as conservative. We put a full ANSYS calculations on hold for the time being.

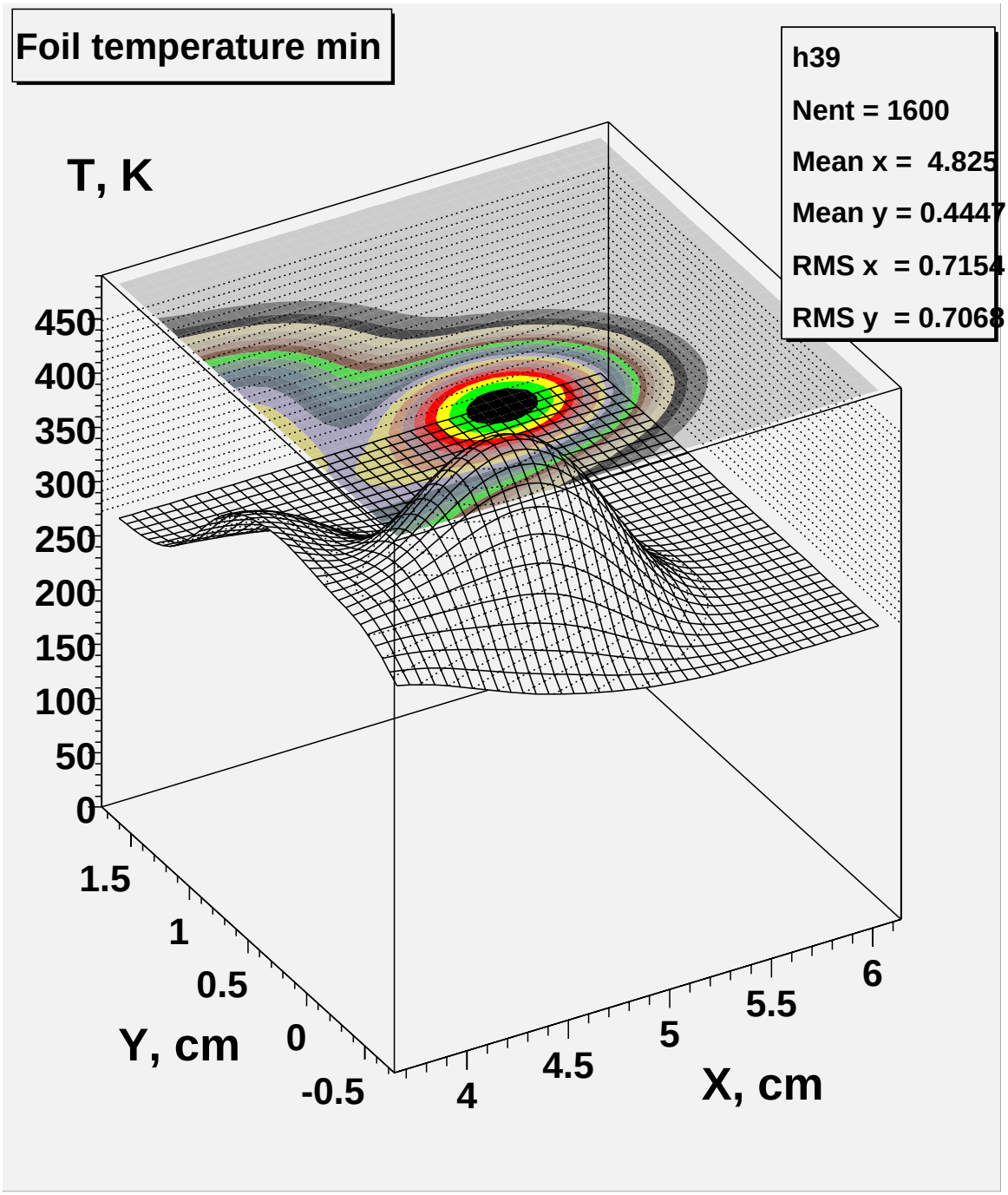

Figure 11.12. Steady state minimum temperature distribution in the stripping foil at painting injection to the proton driver.

11.3.3. Stripping Efficiency, Yield of Excited States $H^o(n)$ Atoms and Beam Dump

Most of injected H^- are stripped to protons in the foil and the rest into excited state of $H^o(n)$ atoms, where n is the principal quantum number of the excited state. Some excited states are field-stripped into protons on the way to the H^o dump. Those particles become a beam

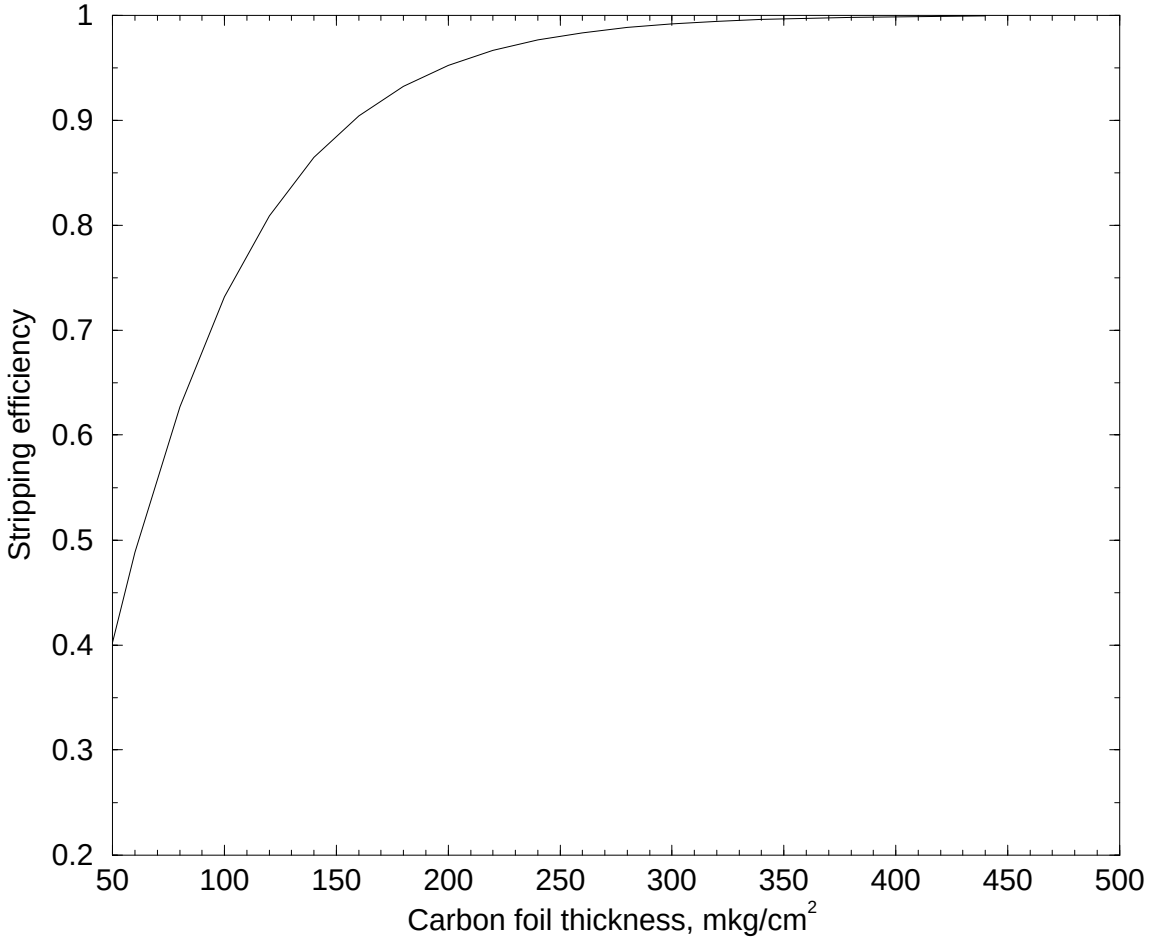

Figure 11.13. Carbon foil stripping efficiency.

halo, and are lost somewhere else in the ring or are intercepted by the collimation system. Defining σ_{if} as the cross-section for the process $H^i \rightarrow H^f + (f-i)e^-$ we can write the stripping efficiency (Fig. 11.3):

$$N_+ = 1 - \frac{\sigma_{-10}\exp\{-\sigma_{01}x\} - (\sigma_{01}-\sigma_{-11})\exp\{-(\sigma_{-10}+\sigma_{-11})x\}}{\sigma_{-10}+\sigma_{-11}-\sigma_{01}}$$

The number of $H^o(n)$ atoms in a highly excited state ($n \geq n_{ex}$), assuming the yield of excited state is proportional to n^{-3}, can be written:

$$Y(n \geq n_{ex}) = (1-N_+)\cdot\frac{\sum_{n=n_{ex}}^{\infty} n^{-3}}{\sum_{n=1}^{\infty} n^{-3}} = (1-N_+)\cdot\frac{\psi'(n_{ex})}{\psi'(1)}$$

We can estimate the foil stripping efficiency, the proton hit distribution and foil temperature after 400 MeV proton beam injection into the machine during 27 turns followed by beam removal from the foil during 6 turns.

The calculations are done with the following assumptions:

1. Electrons are stripped immediately and then pass through the foil independently;

2. Nuclear interactions in the foil are negligible; therefore the main energy deposition sources for a very thin foil are proton restricted ionization energy loss $-\frac{dE_p}{dz}\cdot\frac{\Delta z}{<\cos\theta_p>}\simeq -\frac{dE_p}{dz}\cdot\Delta z$ and electron energy loss during the stripping phase $-2\frac{dE_e}{dz}\cdot\frac{\Delta z}{<\cos\theta_e>}$. Here Δz is foil thickness and $<\cos\theta_p>\simeq 1$ and $<\cos\theta_e>$ are proton and electron angles at stripping.
3. At the kinetic energy of ≈ 218 keV for electrons accompanying this process, the range and $-\frac{dE_e}{dx}$ according to the ICRU37 are $580\cdot 10^2\frac{\mu g}{cm^2}$ and $2.4\frac{MeV\cdot cm^2}{g}$ respectively. Therefore we assume the electron contribution to the heating is approximately equal to -$2\frac{dE_e}{dx}\Delta s_e$.

For carbon foil parameters:

- density $\rho = 2.0\frac{g}{cm^3}$
- thickness $\Delta z = 300\frac{\mu g}{cm^2}$
- specific heat $c_p = 0.165\frac{cal}{g\cdot K}$
- thermal conductivity $\kappa = 0.057\frac{cal}{cm\cdot K\cdot sec}$
- emissivity $\varepsilon = 0.80$,

The calculated stripping efficiency is 99.2% and the estimated yield of excited states $H^o(n)$ atoms with $n \geq 5$ is equal to 0.016%. These atoms will be stripped into protons before they reach the dump and become a beam halo. The remaining excited atoms ($n \leq 4$) have a longer lifetime and they will go to the neutral beam dump.

The average number of proton hits on the foil (1.98) found from simulations is very close to that was calculated analytically (1.95).

The proton hit distribution calculated from the above formulas (Fig. 11.9) was used for foil temperature buildup and steady state temperature calculations.

Due to fairly large size of H^- beam at the foil, the small number of collisions and the small electron contribution, the temperature buildup in the foil per pulse is less than 100K (Fig. 11.10).

The heat emission cooling of the foil due to the Stefan-Boltzmann law

$$Q = \varepsilon\cdot\sigma_{SB}\cdot T^4$$

at this temperature is small. With only emission as a cooling mechanism the foil temperature reaches a steady state after about 10 pulses with maximum temperature of 540 K (Fig. 11.11) and minimum around 450 K (Fig. 11.12).

11.4. Septum and Kicker Magnets Parameters

Septum and kicker magnets parameters are presented in Table 11.2. The septum is curved to reduce the poletip width.

11.5. Stripping Foil Design

Table 11.2. Septum and kicker magnets parameters.

Element	Field	Current	Inductance	Length	Poletip width	Poletip gap	Turns number
Name	Gauss	Amps	μH	m	mm	mm	
septum-magnet	3180	11268	2.99	2	45	45	1
kicker-1	128	176.3	47.87	0.5	180	180	8
kicker-2	212	292.0	47.87	0.5	180	180	8
kicker-3	96	132.2	47.87	0.5	180	180	8
kicker-4	157	216.2	47.87	0.5	180	180	8

Carbon stripping foils of 300 $\mu g/cm^2$ have been in use in the Booster since the 400 MeV Linac upgrade. Foils of densities between 300 and 600 $\mu g/cm^2$ have been used. No foils have ever been lost because of beam damage. It should be pointed out however that the number of turns that the Booster uses is nominally 10 per beam cycle and the Proton Driver will use up to 27 per beam cycle. The Booster also typically operates at a reduced duty factor, something less than 1 Hz, whereas the Proton Driver will operate at 15 Hz continuously. The Booster operational repetition rate will change in the future with the Boone and NuMI experiments to as high as 10 Hz. It is possible that foil damage may become a factor and will have to be dealt with.

There are two basic concerns with the Proton Driver foils, heat dissipation and type of mount.

The stripping foil will reach temperatures of 540 K (513 F). This temperature may be of concern in the mounting of the foil. The Fermilab Booster foils are simply bonded to a thin copper support with super glue. There has never been any problem with this kind of mounting. However the Booster has never run beam at 15 Hz for sustained periods, so average temperature rise has never been a problem. If the foil actually reaches sustained temperatures this high, another mounting technique may have to be used. Keep in mind that even though the foil may get very hot at the beam location, the foil is exceeding is thin and the amount of heat that will be transmitted to the foil holder will be small. The metal holder will be capable of dissipating a large amount of heat relative to the foil so a simple glue bond may suffice. This is not considered a serious matter however; there are many ways of mounting the foil.

The foil will have two free edges. See Fig. 11.2 for the foil dimensions. This is also of some concern. Carbon foils this thin have a tendency to curl up. If this proves to be the case then the foil may have to be mounted with only 1 free edge such as is done in the Booster. However this means the foil will be approximately twice as long. This is not a desirable thing to do since there would be more interactions of the circulating beam with the foil. On the other hand, if necessary, it can be done.

It is planned to test mount foils and try them out in the Booster. The Booster is an ideal test for any foil mounting technique. Changing foils in the Booster is not hard; typically the foils can be changed in about 4 hours with most of the time being for vacuum pump down. The only criterion is that the foil mount itself cannot be thick. The clearances on the

Booster foil changer are on the order of +/- 3 mm. Testing foils in the Booster allows not only various mounting techniques to be tried but measurements of foil temperature rise with beam could also be done.

11.6. Conclusions

A painting injection system, consisting of two sets of horizontal and vertical kicker magnets, produces the quasi-uniform density distribution of the circulating beam required for the beam space charge effect reduction and emittance preservation at injection.

The calculated stripping efficiency is 99.2%, and the estimated yield of excited $H^o(n)$ atoms with $n \geq 5$ is 0.016%. These atoms contribute protons to the beam halo.

The temperature buildup during the injection pulse and steady state temperature of the foil are calculated from an analytical distribution of proton hits using ANSYS code. An instant temperature buildup, calculated with contributions of multiple collisions, ionization loss from protons and electrons accompanying the stripping process, is a little bit less than 100 K.

With only emission as a cooling mechanism the foil temperature reaches a steady state of $\sim$ 540 K after about 10 cycles of injection, that is, less than 1 second.

References

[1] A. Drozhdin, C Johnstone and N. Mokhov,'16 GeV Proton Driver Beam Collimation System', ICFA Mini-Workshop on High-Intensity, High-Brightness Hadron Beams "Beam Halo and Scraping", Lake Como, Wisconsin, September 1999.

[2] A. Drozhdin, O. Krivosheev, N. Mokhov, "Beam Loss, Collimation and Shielding at the Fermilab Proton Driver", Fermilab–FN–693 (2000).

[3] D. Ritson, 16 GeV Proton Driver Lattice, Private communications, December 1999.

[4] I. Baishev, A. Drozhdin, and N. Mokhov, 'STRUCT Program User's Reference Manual', SSCL–MAN–0034 (1994), http://www-ap.fnal.gov/∼drozhdin/

[5] 'JHF Accelerator Design Study Report', KEK Report 97-16, JHF-97-10, March 1998, p3-67 - 3-71..

[6] Particle Data Group, 1998.

[7] ANSYS v5.5 Manual, 1994.